

Supplementary Information

Chiral carbon dots - a functional domain for tyrosinase Cu active site modulation via remote target interaction

Yurong Ma,^a Mengling Zhang^a, Zhixiong Deng^c, Xiting Wang^a, Hui Huang,^{a} Kai Yang,^{c*} Bing Yuan,^c Yang Liu,^{a*} and Zhenhui Kang^{a,b*}*

^a Institute of Functional Nano & Soft Materials (FUNSOM), Jiangsu Key Laboratory for Carbon-Based Functional Materials & Devices, Soochow University, 199 Ren'ai Road, Suzhou, 215123, Jiangsu, China.

^b Macao Institute of Materials Science and Engineering, Macau University of Science and Technology, Taipa 999078, Macau SAR, China.

^c Center for Soft Condensed Matter Physics and Interdisciplinary Research & School of Physical Science and Technology, Soochow University, Suzhou, 215006, China.

*Correspondence to: hhuang0618@suda.edu.cn, yangl@suda.edu.cn,
yangkai@suda.edu.cn, zhkang@suda.edu.cn

Table of Contents

Experimental Section

Figure S1. TEM images and histograms of DLS of (a) LCDs-2, (c) DCDs-1, (D) DCDs-2, (e) DCDs-3.

Figure S2. XPS full scan spectra, high-resolution C 1s XPS spectra, N 1s XPS spectra of (a) LCDs-1, (b) LCDs-2 and (c) LCDs-3.

Figure S3. XPS full scan spectra, high-resolution C 1s XPS spectra, N 1s XPS spectra of (a) DCDs-1, (b) DCDs-2 and (c) DCDs-3.

Figure S4. The FTIR spectra of LCDs-2 (black line), DCDs-2 (red line), LCDs-3 (blue line), DCDs-3 (pink line).

Figure S5. UV-vis spectra, PL excitation (pink line), and emission spectra (yellow line) of (a) LCDs-1, (b) LCDs-2, (c) LCDs-3, (d) DCDs-1, (e) DCDs-2 and (f) DCDs-3.

Figure S6. Viability of 293T cells after 24 h of incubation with different concentrations of L/DCDs-1, L/DCDs-2 and L/DCDs-3.

Figure S7. The histogram of inhibition ratio with different concentrations of citric acid and CDs from citric acid.

Figure S8. The histogram of inhibition ratio with different concentrations of (a) L/D-Asp. Reversible inhibition and irreversible inhibition test of (b) L-Asp, (c) D-Asp. (d) Lineweaver-Burk plots of tyrosinase (black line), tyrosinase/L-Asp (red line), and tyrosinase/D-Asp (blue line). (L/DCDs: 400 $\mu\text{g}/\text{mL}$, tyrosinase: 50 U/mL).

Figure S9. The combination of LCDs-1 or DCDs-1 with tyrosinase. (a) The SDS-PAGE, (b) hydrodynamic diameters, (c) PL spectra ($\lambda_{\text{ex}} = 370 \text{ nm}$).

Figure S10. The structures of L/D-Asp and monolayer L/DCDs-1.

Figure S11. Time series of root mean square deviation (RMSD) of backbone atoms of the protein with respect to the crystal structure when interacting with L/D-Asp.

Figure S12. Time series of root mean square deviation (RMSD) of backbone atoms of the protein with respect to the crystal structure when interacting with L/DCDs-1.

Figure S13. Contribution of top 10 principal components to the structural variance.

Figure S14. Time series of distance between copper ions and the center of mass of the active center (six histidines) of tyrosinase when interacting with (a) DCDs-1 and (b) LCDs-1.

Table S1. The element contents of LCDs-1, LCDs-2, LCDs-3, DCDs-1, DCDs-2 and DCDs-3.

Table S2. The Michaelis constants (V_{\max} and K_m) of tyrosinase, tyrosinase/LCDs-1, tyrosinase/DCDs-1, tyrosinase/LCDs-2, tyrosinase/DCDs-2, tyrosinase/LCDs-3 and tyrosinase/DCDs-3

Experimental Section

Materials. All reagents were purchased from Sigma-Aldrich (Beijing, China) and used as is. Sigma supplied L-/D-asp. Cellulose dialysis bag (500-1000Da) was bought from Shanghai Yuanye Biotechnology Co.Ltd.

Characterization. A FEI/Philips Tecnai G2 F20 TWIN TEM was used to conduct the transmission electron microscopy (TEM) and high-resolution transmission electron microscope (HR-TEM) examination. The X-ray photoelectron spectroscopy (XPS) spectra were got with a KRATOS Axis ultra-DLD X-ray photoelectron spectrometer. The FTIR spectrum was accessed using a Bruker Fourier Transform Infrared Spectrometer (Hyperion). The UV-Vis absorption was measured with a Perkin Elmer Lambda 750 spectrophotometer, and the PL spectra were obtained with a Horiba Jobin Yvon (Fluoro Max-4) luminescence spectrometer. The CD spectra were acquired by using a JASCO J-815 spectropolarimeter. The dynamic light scattering measurement was obtained via utilizing a ZEN3690 zetasizer (Malvern, U.K.).

Synthesis of chiral CDs. For LCDs, 10 g citric acid was heated in round-bottom flask under 180 °C for 50 min and 6 g L-Asp were then added under the same temperature for 30 min, 60 min and 90 min respectively. The amount of water was added to dissolve it and the solution cooled to room temperature naturally. The obtained solution was purified by 500-1000 Da cellulose dialysis membrane for 3 days. The obtained LCDs are named LCDs-1, LCDs-2 and LCDs-3. The synthesis method of DCDs with 30 min (DCDs-1), 60 min (DCDs-2) and 90 min (DCDs-3) was consistent with it (with D-Asp as raw material). Finally, the obtained chiral CDs are stored for further use.

Preparation of tyrosinase/chiral CDs hybrids. For the tyrosinase/LCDs hybrids, 25 KU tyrosinase was first dissolved in 20 mL phosphate buffer solution (PBS, 0.02 mol/L, pH=6.8). Then, 10 μ L tyrosinase solution was mixed with 115 μ L different concentrations (0-600 μ g/mL) of L/DCDs for 2 h at 30 °C for further

use. The tyrosinase/DCDs hybrids were fabricated with the same method as above.

Activity assays of tyrosinase and tyrosinase/CDs. In this assay, activities of mushroom tyrosinase were determined as previously reported¹ with modification. L-dopa was selected as substrate and 125 μL L-DOPA (5 mM) solution was added to the tyrosinase and tyrosinase/CDs hybrids solution above (total volume: 250 μL). Then the resulting solution was immediately tested per minute to obtain absorbance at 475 nm for 10 min at 30 °C. All assays should be run at least three times to reduce errors. The inhibition rate can be calculated by the following formula:

$$\text{Inhibition ratio} = (OD_{control} - OD_{sample}) / OD_{control} \times 100\%$$

Herein, $OD_{control}$ and OD_{sample} represent the absorbance of tyrosinase and tyrosinase/CDs hybrids at 475 nm.

The analysis of Michaelis - Menten equation for tyrosinase. The Michaelis - Menten equation analysis was obtained via consulting the method previously described.² To determine whether CDs were irreversible or reversible, a certain amount of inhibitors CDs (0, 200, 400 and 600 $\mu\text{g}/\text{mL}$) were added to the different concentration (25, 50, 75 and 100 U/mL) of tyrosinase (E). Then the initial reaction rates (v) of different tyrosinase concentrations were determined. Plot the v versus E to analyze the reversible or irreversible inhibition. To judge the classification of CDs in reversible inhibitors, a series concentration of substrate (0.25, 0.5, 0.75 and 1 μM) reacted with tyrosinase and tyrosinase/CDs hybrid enzymes and the different initial reaction rates of different concentrations were determined respectively. The Lineweaver-Burk plot was accessed by plotting the $1/V$ (the reciprocal of initial reaction rate) versus $1/[S]$ (the reciprocal of the concentration of substrate). And then, the Y-intercept symbolizes $1/V_{max}$ and the X-intercept represents $-1/K_m$, respectively, so that the value of V_{max} and K_m were obtained.

SDS-polyacrylamide gel electrophoresis (SDS-PAGE). SDS-PAGE (w/w: 8%) was used to separate tyrosinase and tyrosinase/CDs hybrids (tyrosinase: 500 U/mL, LCDs or DCDs: 4 mg/mL) in a sample loading buffer containing 1% lithium dodecyl sulfate and 1% β -mercaptoethanol (constant voltage: 80 V, 2 h). Afterwards the gel was stained with Coomassie Brilliant Blue R-250 (0.25 percent).³

In vitro cytotoxicity analysis. The human embryonic kidney (HEK) 293T cell lines were incubated in standard medium in 5 % CO₂ atmosphere at 37 °C. The cells were grown on a 96-well plate for 24 hours before being exposed to various doses of L/DCDs (0, 100, 200, 300, 400, 500, and 600 g/mL) to determine cytotoxicity. Then the cytotoxicity of L/DCDs was determined by cell counting kit-8 (CCK8). The absorbance at 450 nm was tested by a microplate reader (Bio-Rad 680, USA). All measurements were repeated at least three times to prove the credibility.

Molecular dynamics simulations. All molecular dynamics simulations were conducted with Gromacs⁴ v.2019.4 simulation engine under Charmm 36 force field parameters and topologies.⁵ The atomic model of CDs is downloaded from Charmm-GUI webserver.⁶ The 3D atomic models of D/L-aspartic acid are downloaded from PubChem and then uploaded to the CGenFF webserver to obtain simulation parameters.⁷ The systems contain 20 L/DCDs or 80 L/D-aspartic acids, 14,275 TIP3P water molecules, 46 sodium and 49 chloride ions. After initial energy minimizations, both systems were equilibrated for 10 ns, followed by production runs of up to 1 μ s. The cut-off for contact probability is set to 0.4 nm. The analysis of PCA and ANM modes were assessed using the ProDy package.^{8,9}

References

1. L. Qiu, Q. H. Chen, J. Zhuang, X. Zhong, J. Zhou, Y. Guo and Q. X. Chen, *Food Chem.*, 2009, **112**, 609-613.
2. S. Guo, H. Li, J. Liu, Y. Yang, W. Kong, S. Qiao, H. Huang, Y. Liu and Z. Kang, *ACS Appl. Mater. Interfaces*, 2015, **7**, 20937-20944.
3. H. Li, S. Guo, C. Li, H. Huang, Y. Liu and Z. Kang, *ACS Appl. Mater. Interfaces*, 2015, **7**, 10004-10012.
4. M. J. Abraham, T. Murtola, R. Schulz, S. Páll, J. C. Smith, B. Hess and E. Lindahl, *SoftwareX*, 2015, **1-2**, 19-25.
5. J. Huang and A. D. MacKerell, Jr., *J. Comput. Chem.*, 2013, **34**, 2135-2145.
6. S. Jo, T. Kim, V. G. Iyer and W. Im, *J. Comput. Chem.*, 2008, **29**, 1859-1865.
7. K. Vanommeslaeghe, E. Hatcher, C. Acharya, S. Kundu, S. Zhong, J. Shim, E. Darian, O. Guvench, P. Lopes, I. Vorobyov and A. D. Mackerell, Jr., *J. Comput. Chem*, 2010, **31**, 671-690.
8. A. Bakan, L. M. Meireles and I. Bahar, *Bioinformatics*, 2011, **27**, 1575-1577.
9. Ahmet Bakan and I. Bahar., *PNAS*, 2009, **106**, 14349-14354.

Supplementary Figures

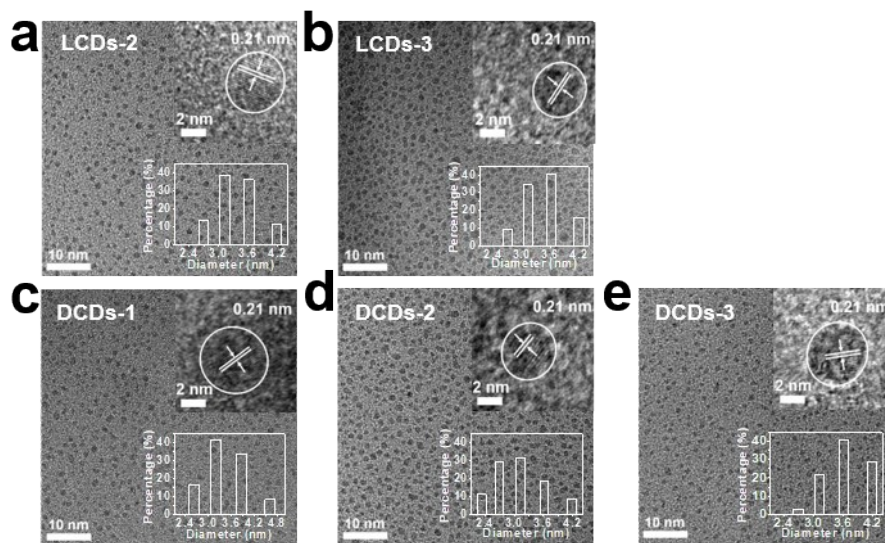


Figure S1. TEM images and histograms of DLS of (a) LCDs-2, (c) DCDs-1, (D) DCDs-2, (e) DCDs-3.

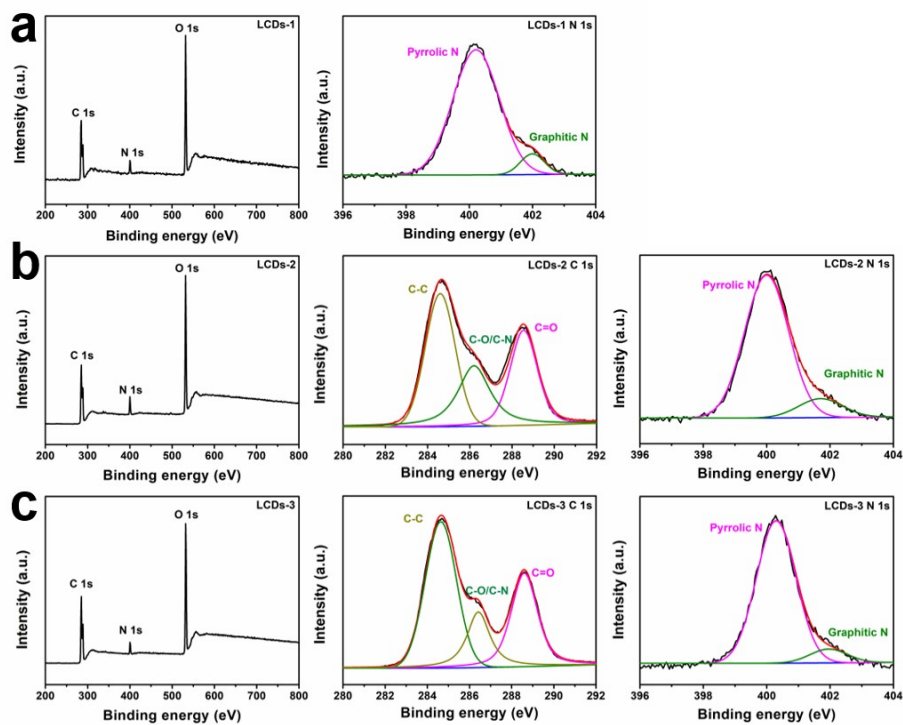


Figure S2. XPS full scan spectra, high-resolution C 1s XPS spectra, N 1s XPS spectra of (a) LCDs-1, (b) LCDs-2 and (c) LCDs-3.

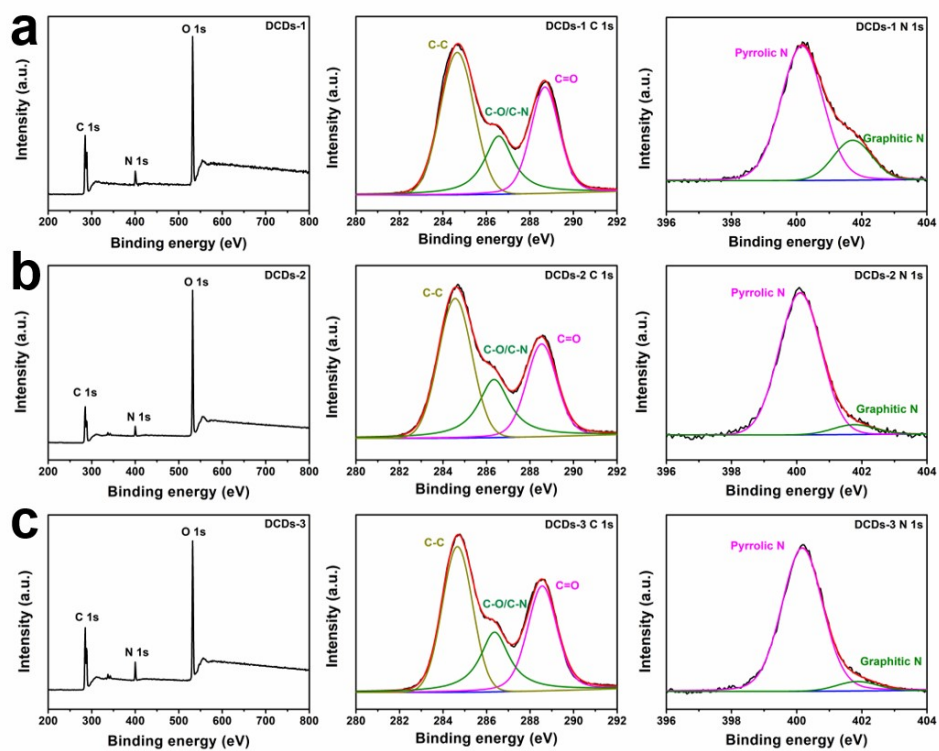


Figure S3. XPS full scan spectra, high-resolution C 1s XPS spectra, N 1s XPS spectra of (a) DCDs-1, (b) DCDs-2 and (c) DCDs-3.

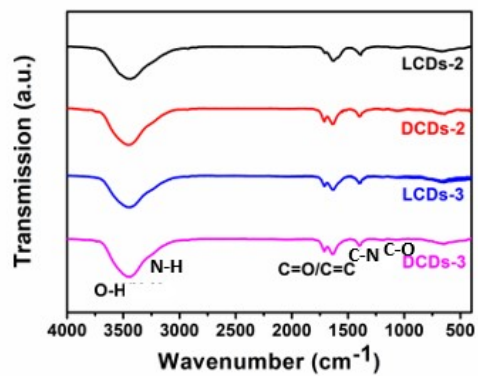


Figure S4. The FTIR spectra of LCDs-2 (black line), DCDs-2 (red line), LCDs-3 (blue line), DCDs-3 (pink line).

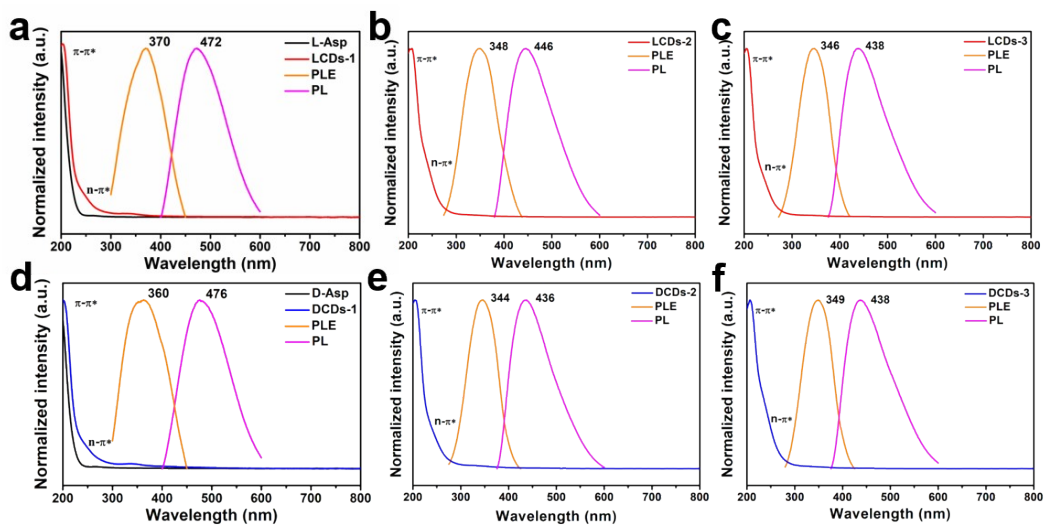


Figure S5. UV-vis spectra, PL excitation (pink line), and emission spectra (yellow line) of (a) LCDs-1, (b) LCDs-2, (c) LCDs-3, (d) DCDs-1, (e) DCDs-2 and (f) DCDs-3.

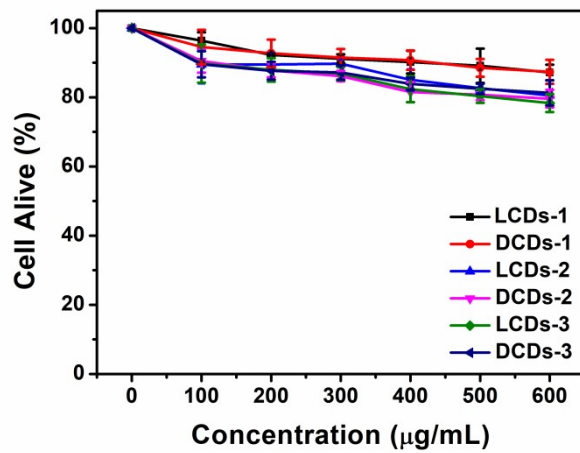


Figure S6. Viability of 293T cells after 24 h of incubation with different concentrations of L/DCDs-1, L/DCDs-2 and L/DCDs-3.

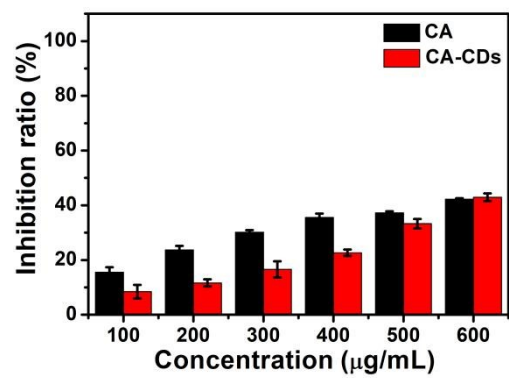


Figure S7. The histogram of inhibition ratio with different concentrations of citric acid and CDs from citric acid.

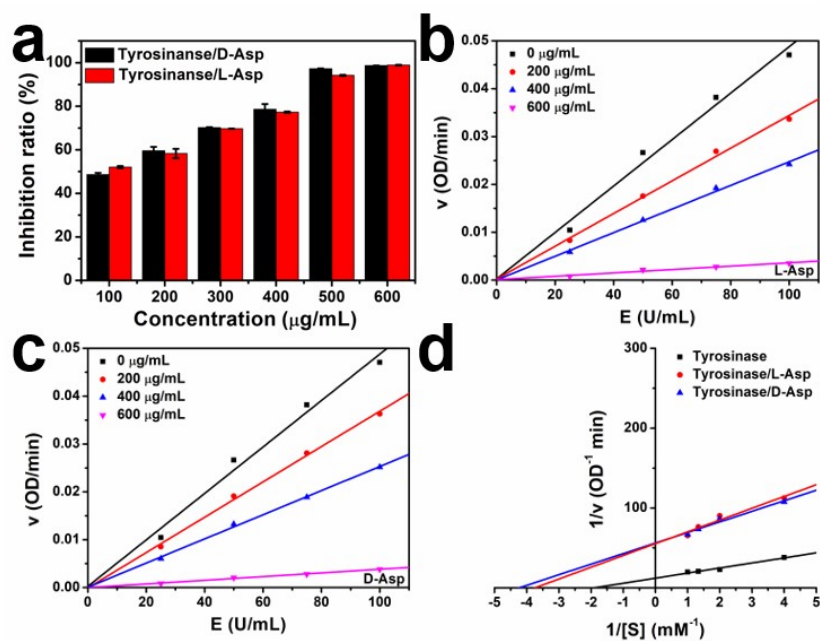


Figure S8. The histogram of inhibition ratio with different concentrations of (a) L/D-Asp. Reversible inhibition and irreversible inhibition test of (b) L-Asp, (c) D-Asp. (d) Lineweaver-Burk plots of tyrosinase (black line), tyrosinase/L-Asp (red line), and tyrosinase/D-Asp (blue line). (L/DCDs: 400 μg/mL, tyrosinase: 50 U/mL).

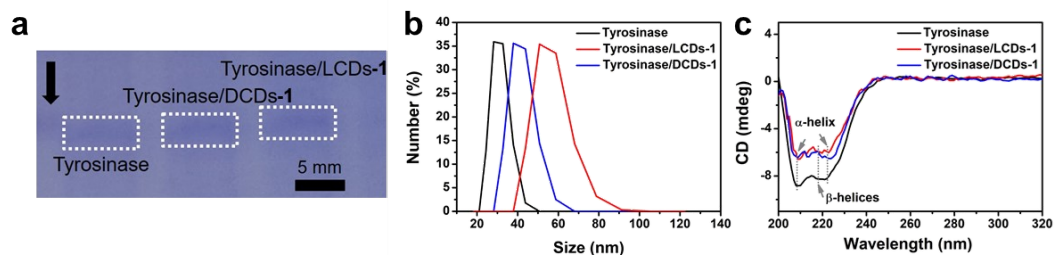


Figure S9. The combination of LCDs-1 or DCDs-1 with tyrosinase. (a) The SDS-PAGE, (b) hydrodynamic diameters, (c) PL spectra ($\lambda_{\text{exc}} = 370 \text{ nm}$).

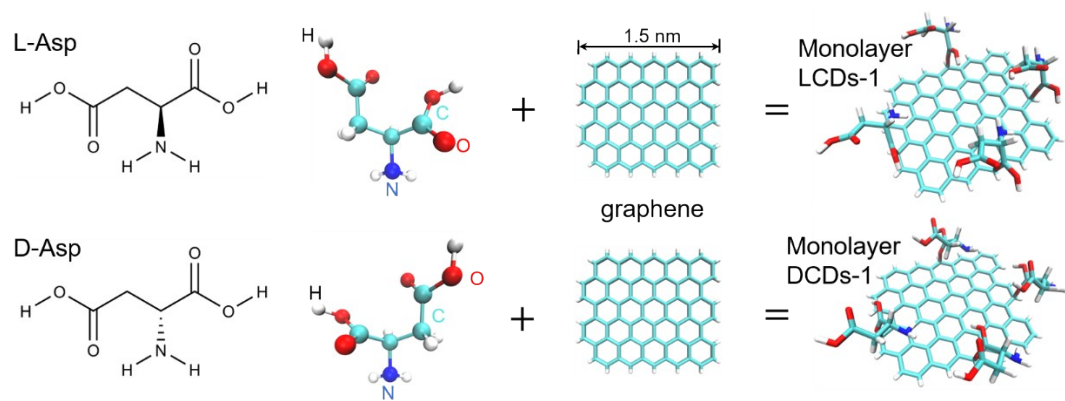


Figure S10. The structures of L/D-Asp and monolayer L/DCDs-1.

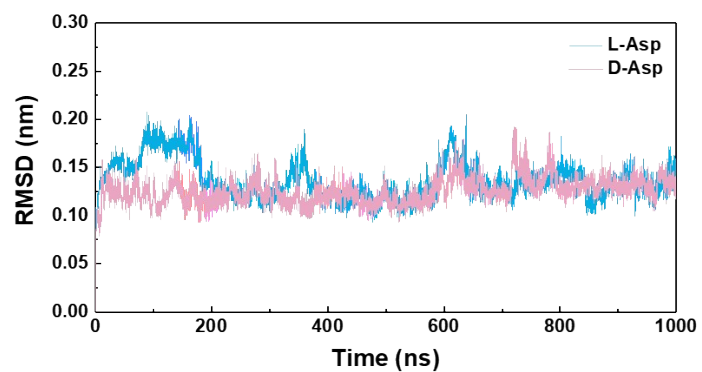


Figure S11. Time series of root mean square deviation (RMSD) of backbone atoms of the protein with respect to the crystal structure when interacting with L/D-Asp.

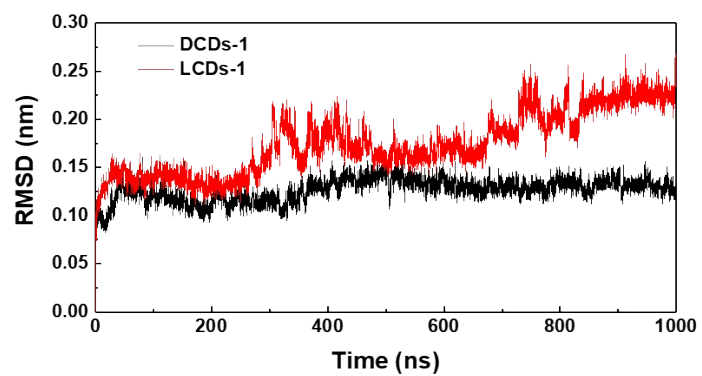


Figure S12. Time series of root mean square deviation (RMSD) of backbone atoms of the protein with respect to the crystal structure when interacting with L/DCDs-1.

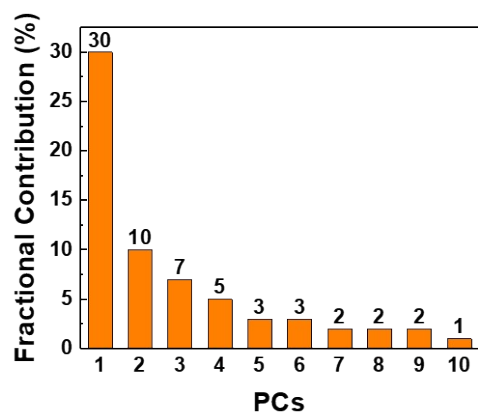


Figure S13. Contribution of top 10 principal components to the structural variance.

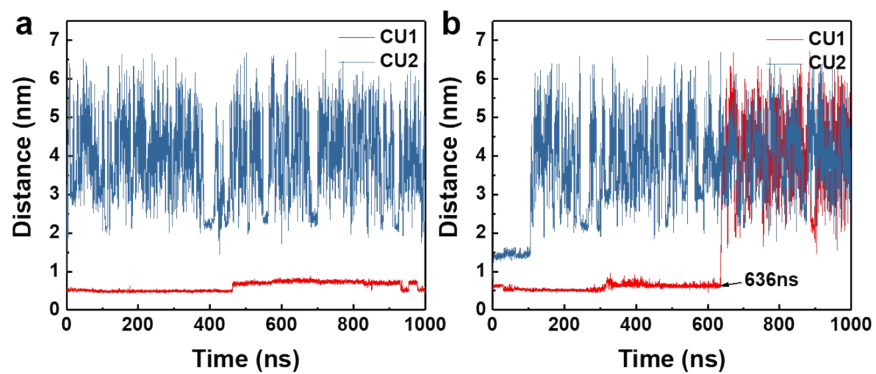


Figure S14. Time series of distance between copper ions and the center of mass of the active center (six histidines) of tyrosinase when interacting with (a) DCDS-1 and (b) LCDs-1.

Supplementary Tables

Table S1. The average size, zeta potential, element contents and cell alive of LCDs-1, LCDs-2, LCDs-3, DCDS-1, DCDS-2 and DCDS-3.

	LCDs-1	LCDs-2	LCDs-3	DCDS-1	DCDS-2	DCDS-3
Average size (nm)	3.44	3.36	3.45	2.99	3.09	3.40
Zeta potential (eV)	-18.1	-12.7	-8.19	-19.8	-11.4	-11.2
C (%)	57.99	57.97	57.97	48.59	55.15	58.28
N (%)	5.98	6.68	6.68	4.66	5.41	6.01
O (%)	36.03	35.35	35.35	46.74	39.44	35.71
Cell alive (%)	87.14	80.48	78.33	87.33	79.59	81.26

Table S2. The Michaelis constants (V_{\max} and K_m) of tyrosinase, tyrosinase/LCDs-1, tyrosinase/D CDs-1, tyrosinase/LCDs-2, tyrosinase/D CDs-2, tyrosinase/LCDs-3 and tyrosinase/D CDs-3.

Enzyme	V_{\max} (OD/min)	K_m (mM)
Tyrosinase	0.08	0.52
Tyrosinase/LCDs-1	0.03	1.58
Tyrosinase/D CDs-1	0.05	0.38
Tyrosinase/LCDs-2	0.02	0.52
Tyrosinase/D CDs-2	0.01	0.31
Tyrosinase/LCDs-3	0.02	0.48
Tyrosinase/D CDs-3	0.02	0.52